J Biol Inorg Chem
DOI 10.1007/s00775-015-1280-4

ORIGINAL PAPER

Water-soluble lipophilic MR contrast agents for cell membrane labeling

Christiane E. Carney[1] · Keith W. MacRenaris[1] · Thomas J. Meade[1]

Received: 18 May 2015 / Accepted: 27 June 2015

Abstract Long-term cell tracking using MR imaging necessitates the development of contrast agents that both label and are retained by cells. One promising strategy for long-term cell labeling is the development of lipophilic Gd(III)-based contrast agents that anchor into the cell membrane. We have previously reported the efficacy of monomeric and multimeric lipophilic agents and showed that the monomeric agents have improved labeling and contrast enhancement of cell populations. Here, we report on the synthesis, characterization, and in vitro testing of a series of monomeric lipophilic contrast agents with varied alkyl chain compositions. We show that these agents disperse in water, localize to the cell membrane, and label HeLa and MCF7 cells effectively. Additionally, these agents have up to tenfold improved retention in cells compared to clinically available ProHance®.

Keywords MRI · Contrast agents · Gadolinium · Cell membrane · Cell labeling

Introduction

Cell transplantation has been implicated as a potential therapeutic strategy for the treatment of conditions such as cancer [1], cardiovascular [2, 3], and degenerative diseases [4, 5]. One significant challenge with cell transplantation therapy is the need to monitor the location and distribution of transplanted cells over time [6, 7]. MRI is ideally suited for serial imaging of transplanted cells since it does not require ionizing radiation or radiotracers like CT, PET, and SPECT. Additionally, MRI provides high spatial and temporal resolution with unlimited penetration depth. Intrinsic MR contrast can be enhanced using paramagnetic contrast agents with Gd(III)-based complexes the most commonly used in the clinic [8]. These agents generate positive (bright) image contrast by decreasing the proton spin lattice relaxation time (T_1) of surrounding water protons [9]. The efficacy of a contrast agent is defined by its relaxivity (r_1) which reflects its ability to shorten the T_1 of water protons.

For Gd(III)-based contrast agents to be used in longitudinal cell tracking studies, new probes must be developed that label cells with high levels of Gd(III) and remain associated with cells for long periods of time. Agents developed for this application have included small molecules [10], peptides [11–13], polymers [14–16], and nanoparticles [17]. All of these contrast agents are internalized by cells which can result in endosomal entrapment that in turn can lead to relaxivity quenching and contrast agent degradation [18, 19]. This may limit the amount of time labeled cells remain detectable by MRI.

An alternate strategy for long-term cell labeling is the development of lipophilic contrast agents that anchor into the cell membrane without cellular internalization. This strategy has been used for decades in optical imaging with dyes such as DiO and DiA. The first reported

Electronic supplementary material The online version of this article (doi:10.1007/s00775-015-1280-4) contains supplementary material, which is available to authorized users.

✉ Thomas J. Meade
tmeade@northwestern.edu

[1] Department of Chemistry, Molecular Biosciences, Neurobiology, Biomedical Engineering, and Radiology, Northwestern University, 2145 Sheridan Road, Evanston, IL 60208-3113, USA

Published online: 28 July 2015

membrane-anchored MR contrast agent involved conjugating alkyl chains to a Gd(III) complex [20]. The resulting agent labeled cells at low incubation concentrations and showed potential for long-term imaging. Our lab continued the development of lipophilic contrast agents by comparing the labeling and retention of monomeric (contains one Gd(III) complex) and multimeric (contains three Gd(III) complexes) agents [21]. We showed that the monomeric agent had the surprising ability to label cells more effectively and produce more significant contrast enhancement than the multimeric counterpart. Further, the monomeric agent had improved solubility and did not require incubation with detergent in biological media, a limitation of the multimeric design. Herein, we further develop the design of monomeric lipophilic Gd(III) contrast agents that contain a thermodynamically and kinetically stable macrocyclic chelate. We vary the alkyl chain composition of the chelate and investigate the effect on cell labeling and retention.

Materials and methods

Synthetic methods

Alkyne-modified Gd(III) chelate (**8**) [22] and compounds **6** [23], **9** [24], **11** [25], and **12** [25] were synthesized according to the literature procedures. See the Supporting Information for synthetic procedures of new compounds.

Log*P* measurements

Approximately 1 mg of complexes **1**–**5** were dissolved in 1 mL of 1:1 water:octanol. The samples were vortexed and placed on a rotator for 14 h of mixing. Samples were removed from the rotator and allowed to equilibrate for 12 h. An aliquot was removed from each layer and analyzed for Gd(III) content by ICP-MS. The partition coefficient was calculated from the following equation: $\log_{10} P = \log_{10}(C_o/C_w)$, C_o is the concentration of Gd(III) in the octanol layer and C_w is the concentration of Gd(III) in the water layer.

Determination of CMC

A Nile red assay was used to determine CMC. Solutions of **1**–**5** ranging 0–30 μM were prepared in DPBS. To each was added 2 μL of Nile red stock solution (150 μM in ethanol) to yield a total volume of 1 mL. Fluorescence emission spectra were recorded using a Hitachi F-45000 Fluorescence Spectrophotometer with an excitation wavelength of 550 nm. The excitation slit width, emission slit width and photomultiplier voltages were 10, 10 nm, and 700 V, respectively. The CMC was determined to be the lowest concentration that caused a blue shift in emission of the Nile red. Concentrations of **1**–**5** were verified using ICP-MS.

ICP-MS

The Gd(III) content of relaxivity solutions, log*P* solutions, and cell suspensions was determined using ICP-MS according to an established procedure [21].

Dynamic light scattering (DLS)

Solutions of **1**–**5** were prepared at 1 mM and filtered through 0.2 μm filters into SARSTEDT clear polystyrene 10 × 10 × 45-mm cuvettes. Data were acquired on a Malvern Instruments Zetasizer Nano Series Nano-ZS equipped with Dispersion Technology Software v5.03 (Worcestershire, United Kingdom).

Cell culture methods

HeLa (ATCC® CCL-2™) and MCF7 (ATCC® HTB-22) were purchased from the American Type Culture Collection (Manassas, VA, USA). HeLa cells were cultured in phenol red-free minimum essential media (MEM) supplemented with 10 % fetal bovine serum (FBS). MCF7 cells were cultured in RPMI medium 1640 supplemented with 10 % FBS. Cells were plated and incubated for 24 h before all experiments. Doses were filtered through 0.2 μm sterile filters prior to administration. Cells were harvested using 0.25 % TrypLE.

Cell counting and viability

A Guava EasyCyte Mini Personal Cell Analyzer (EMD Millipore, Billerica, MA) was used to count cells and determine viability after labeling experiments. Briefly, cells were harvested and an aliquot of the cell suspension was mixed with Guava ViaCount reagent to reach a total volume of 200 μL. The viability and cell count was determined using ViaCount module software. Cell viability was confirmed using a CellTiter 96® AQueous Non-Radioactive Cell Proliferation Assay (Promega, Madison, WI) where cells were plated in 96-well plates at a density of 5000 cells per well. Cells were incubated with various concentrations of **1**–**5** for 24 h. The assay was then carried out according to the manufacturer's protocol. IC_{50} values were determined using GraphPad Prism software (La Jolla, CA, USA).

Cellular labeling studies

Labeling studies were performed with HeLa and MCF7 cell lines with 25,000–30,000 cells plated in each well

of a 24-well plate. For concentration-dependent labeling studies, complexes **1**–**5** were dissolved into media at concentrations of 0–120 μM for **1** and **3**–**5** while complex **2** was dissolved at concentrations of 0–40 μM (180 μL dose). For time-dependent labeling studies, cells were incubated with 35 μM of **1**–**5** for 1, 2, 4, 8, and 24 h. Cells were harvested according to previously described procedures [21].

Mechanism of cell labeling

Mechanism of labeling studies was performed with HeLa cells with 35,000 cells plated in each well of a 24-well plate. Cells were incubated with one of the following inhibitors or media (control): 0.00275 % poly-L-lysine, 250 μM amiloride, 25 μM chlorpromazine, 5 μM filipin (180 μL dose). After a 30-min incubation, 20 μL of a 10X solution of **1**–**5** or ProHance was added to each well and incubated an additional 4 h. Cells were harvested as described in the cell labeling section. Statistical significance was determined using GraphPad Prism software.

Cell retention

Retention was determined in HeLa and MCF7 cells with 50,000–60,000 cells plated in each well of a 12-well plate. Cells were incubated with various concentrations of **1**–**5** and ProHance® chosen to equalize cell labeling for 24 h (600 μL dose). Cells were harvested according to previously described procedures [21].

Low-field relaxivity (r_1)

Relaxivity at 1.41 T was determined using a Bruker mq60 minispec NMR spectrometer (Bruker Canada; Milton, Ontario, Canada) using solutions of **1**–**5** prepared in DPBS at concentrations of 1 mM and serially diluted four times.

Cell pellet and solution MR imaging

Cell pellet images and high-field relaxivity were determined at 7 T according to previously described methods using a Bruker Pharmscan 7 T imaging spectrometer [21]. Briefly, a rapid-acquisition rapid-echo (RARE-VTR) T_1-map pulse sequence with static TE (11 ms), variable TR (150, 250, 500, 750, 1000, 2000, 4000, 6000, 8000, and 10,000 ms) values, field of view (FOV) = 25 × 25 mm^2, matrix size (MTX) = 256 × 256, number of axial slices = 4, slice thickness (SI) = 1.0 mm, and averages (NEX) = 3 was used.

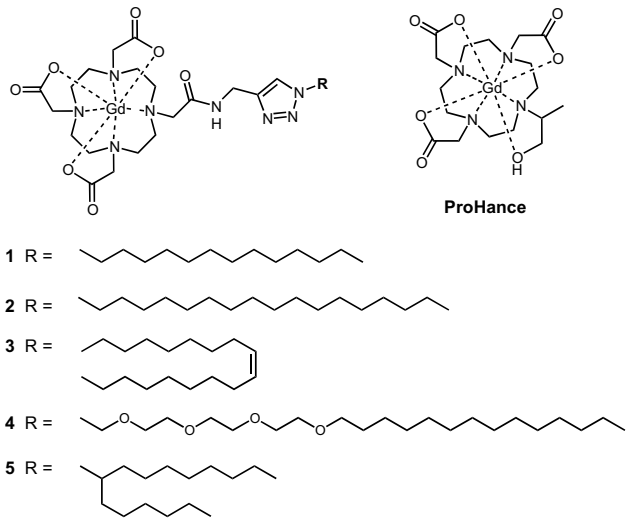

Fig. 1 Lipophilic MR contrast agents **1**–**5** contain alkyl chains of various lengths and branching. Complexes were synthesized with click chemistry and contain the same Gd(III) chelate. ProHance®, a clinically approved contrast agent, was used as a control

Results and discussion

Synthesis and characterization of complexes

A series of lipophilic MR contrast agents was synthesized to contain various alkyl chains conjugated to the same Gd(III) chelate via 'click' chemistry (Fig. 1). Complexes **1** and **2** were synthesized according to Scheme S1. Brominated alkyl chains were converted to the azide and clicked to alkyne-modified chelate (**8**) in 2:1 ^{t}BuOH:H_2O with $CuSO_4$ and sodium ascorbate. The final products contained alkyl tails of 14-carbons (**1**) and 18-carbons (**2**). Complex **3** was synthesized to contain an unsaturated 18-carbon tail according to Scheme S2. Specifically, oleyl alcohol was brominated using CBr_4 and PPh_3 in DCM at 0 °C. Subsequently, the product was converted to the azide and clicked to **8** to afford **3**. Complex **4** was synthesized with a PEG spacer according to Scheme S3. Specifically, tetraethylene glycol was monotosylated and converted to the azide. The PEG spacer was conjugated to 1-bromotetradecane using NaH and KI in DMF at 80 °C. This product was clicked to **8** in 2:1 ^{t}BuOH:H_2O with $CuSO_4$ and sodium ascorbate to afford **4**. Complex **5** was synthesized according to Scheme S4. 2-Hexyldecanol was brominated with *N*-bromosuccinimide, converted to the azide, and clicked to **8** to afford the final product.

The lipophilicity of complexes **1**–**5** was determined by octanol–water partition coefficient (log*P*) measurements (Table 1). Complex **4** was the least lipophilic with a log*P* of −0.01 ± 0.03 while complexes **1** and **5** had similar

Table 1 Characterization of complexes 1–5 including logP, relaxivity, and size measurements

	LogP	r_1 1.41 T, 37 °C (mM^{-1} s^{-1})	r_1 7 T, 25 °C (mM^{-1} s^{-1})	Size (nm)	CMC (μM)
1	0.96 ± 0.03	18 ± 1	4.3 ± 0.1	5.6 ± 0.6	21 ± 1
2	1.20 ± 0.01	19 ± 1	5.2 ± 0.1	6.5 ± 0.2	n/a[a]
3	1.22 ± 0.06	18 ± 1	5.2 ± 0.1	4.3 ± 0.6	5 ± 1
4	−0.01 ± 0.03	11 ± 2	5.1 ± 0.3	7.6 ± 0.8	14 ± 1
5	0.94 ± 0.06	14 ± 2	4.7 ± 0.2	6.4 ± 0.5	22 ± 1

All measurements were made above the CMC of each complex

[a] The CMC was too low to be measured with the Nile red assay (<1 μM)

log*P* values of 0.96 ± 0.03 and 0.94 ± 0.06, respectively. The most lipophilic complexes were **2** and **3** with values of 1.20 ± 0.01 and 1.22 ± 0.06, respectively. Despite the range of log*P* values obtained, all complexes were dispersed in water without detergent, an improvement from our previous generation of multimeric lipophilic agents [21].

Critical micelle concentrations (CMC) were measured using a Nile red assay where complexes **1**–**5** were co-incubated with Nile red dye. Below the CMC of the lipophilic contrast agent, the Nile red emission will match that of the dye alone. Above the CMC, the emission is blue shifted allowing for facile determination of micelle formation [26]. Complexes **2** and **3** had the lowest CMC values of 5 μM and below while complexes **1**, **4**, and **5** had CMC values between 14 and 22 μM (Table 1). Relaxivity measurements and subsequent cell studies were performed at concentrations above the CMC of each complex (except for concentration-dependent uptake). Relaxivity was measured at both low (1.41 T) and high (7 T) magnetic field strengths (Table 1; see Table S1 for r_2 values). At 1.41 T, complex **4** had the lowest relaxivity of 10.5 ± 1.6 mM^{-1} s^{-1} followed by **5** with a relaxivity of 14.4 ± 1.8 mM^{-1} s^{-1}. Complexes **1**, **2**, and **3** had relaxivities of approximately 18 mM^{-1} s^{-1}. At 7 T, relaxivities drop to 4.3–5.2 mM^{-1} s^{-1}. These relaxivity values are attributed to aggregation as measured by DLS. All the agents form micelles in solution ranging from 4 to 8 nm in diameter (Table 1).

Cell labeling and toxicity of lipophilic agents

Cellular labeling of complexes **1**–**5** was investigated in HeLa and MCF7 cells with incubation concentrations that maintained ≥90 % cell viability (see Table 2 for IC_{50} values) for 24 h (Figure S11). In both cell lines, complex **2** with the 18-carbon alkyl tail achieves high labeling (6 fmol Gd(III)/cell for HeLa and 3.7 fmol Gd(III)/cell for MCF7) at 30 μM incubations indicating that it is the most effective complex at low concentrations (Fig. 2). The cytotoxicity of **2** prevents incubations at higher concentrations though the remaining complexes can be incubated at 100–120 μM. This is consistent with other studies that have found a correlation between aliphatic tail length and cytotoxicity [27, 28]. It is likely that the high labeling of **2** perturbs the cell membrane, and results in a lower IC_{50} value compared to the other agents.

In HeLa cells, complexes **1**, **3**, and **4** achieve the same labeling at all concentrations examined. Complex **5** with the 6 and 10 carbon alkyl chains labels cells the least effectively achieving a maximum of 2.6 fmol Gd(III)/cell. In MCF7 cells, **3** labels cells with a maximum of 4.6 fmol Gd(III)/cell followed by **1** (3.6 fmol Gd(III)/cell), **4** (2.1 fmol Gd(III)/cell), and **5** (1.7 fmol Gd(III)/cell). Overall, these results show that **2** is the most effective complex for cell labeling though it is limited by high cytotoxicity. Complexes **1**, **3**, and **4** have similar labeling and lower cytotoxicity than complex **2** making them candidates for further evaluation. Complex **5** is the least effective for cell labeling in both HeLa and MCF7 cell lines likely because the 6- and 10-carbon tails are too short to effectively intercalate into the cell membrane.

Mechanism of cellular labeling

The mechanism of cell labeling for complexes **1**–**5** was investigated in HeLa cells and compared to that of

Table 2 IC_{50} values for **1**–**5** were determined in HeLa cells using an MTS assay

	IC_{50} (mM)
1	0.159 ± 0.022
2	0.076 ± 0.008
3	0.176 ± 0.012
4	0.136 ± 0.03
5	1.22 ± 0.003

Error bars represent ±the standard deviation of the mean of duplicate experiments. The MTS value from each experiment was determined by fitting data from cells treated with 8 concentrations of each complex in triplicate (for a total of 24 wells per experiment)

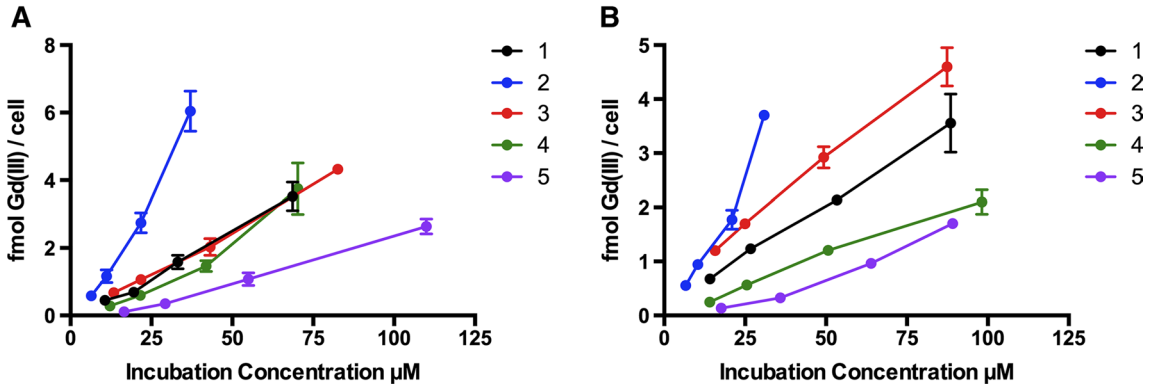

Fig. 2 Concentration-dependent cell labeling of complexes **1**–**5** in **a**. HeLa and **b**. MCF7 cells. These results show that **2** is the most effective complex for cell labeling at low concentrations. Complex **5** is the least effective in both cell lines. The remaining complexes (**1**, **3**, **4**) label cells to a similar degree. *Error bars* ±standard deviation of the mean of triplicate experiments

Table 3 Mechanism of cellular uptake of 1–5 and ProHance® was investigated by co-incubation with various inhibitors in HeLa cells

Inhibitor	Inhibitor of	1	2	3	4	5	ProHance
Poly-L-lysine	Cell membrane	*	*	*	***	*	ns
Amiloride	Macropinocytosis	ns	ns	ns	ns	ns	*
Chlorpromazine	Clathrin	ns	ns	ns	ns	ns	ns
Filipin	Caveolae	ns	ns	ns	ns	**	**
Temperature (4 °C)	Cell membrane fluidity	***	**	***	***	n/a[a]	**

Data show that the lipophilic complexes label the cell membrane while ProHance® is taken up via macropinocytosis and caveolae-mediated endocytosis. Statistical significance from controls was determined using an unpaired t test

ns Not significant

[a] Cell death was observed in cells treated with 5 at 4 °C. This effect was not observed for other complexes or cells treated with 5 and incubated at 37 °C

* $P < 0.05$, ** $P < 0.01$, *** $P < 0.001$

ProHance®, a clinically available contrast agent known to be internalized by cells in cell culture (Table 3) [18]. Experiments were performed according to the literature procedures [29]. To assess the contribution of various endocytotic pathways to labeling, cells were treated with the following inhibitors: poly-L-lysine (disruption of cell membrane associations), amiloride (inhibitor of macropinocytosis), chlorpromazine (inhibitor of clathrin-mediated endocytosis), filipin (disruption of caveolae-mediated endocytosis), and low temperature (disrupts energy-dependent processes and reduces fluidity of cell membrane) for 30 min prior to the addition of **1**–**5** and ProHance®. Cells were then incubated an additional 4 h to allow for contrast agent labeling. The effect of the inhibitor was determined by comparing the labeling to cells treated with **1**–**5** and ProHance® alone. Poly-L-lysine and low temperature (4 °C) were the only inhibitors to cause a statistically significant decrease in labeling for all the lipophilic contrast agents indicating that the complexes label the cell membrane and are not internalized into cells. However, filipin decreased the labeling of **5** indicating at least partial internalization by caveolae-mediated endocytosis. Conversely, the labeling of ProHance® was decreased by amiloride, filipin, and low temperature. This implicates macropinocytosis and caveolae-mediated endocytosis as the mechanisms responsible for cell labeling. This result is consistent with other studies that have found the uptake of ProHance® occurs via macropinocytosis [18, 19].

MR imaging of cell pellets

To assess the ability of **1**–**5** to produce MR contrast enhancement in labeled cells, T_1-weighted images of HeLa cell pellets were acquired at 7 T (Fig. 3). Complexes **2** and **3** produced the greatest contrast enhancement with a 58 % reduction in T_1 compared to untreated cells followed closely by **1** with a 51 % reduction in T_1. Complexes **4** and **5** performed less effectively with a 32 and 20 % reduction in T_1, respectively. No significant enhancement was observed in cells treated with ProHance®. Surprisingly, **3** produces

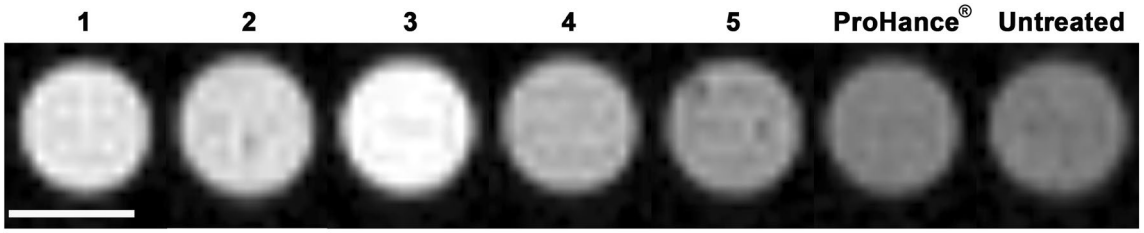

	1	2	3	4	5	Prohance®	Control
Fmol Gd(III) per cell	1.46 ± 0.07	2.44 ± 0.12	1.17 ± 0.06	0.64 ± 0.03	0.48 ± 0.02	0.25 ± 0.01	0.020 ± 0.001
T_1 (ms)	1038 ± 69	867 ± 80	892 ± 82	1443 ± 99	1704 ± 103	2102 ± 119	2132 ± 131

Fig. 3 T_1-weighted HeLa cell pellet images acquired at 7 T of **1**–**5** and ProHance®. *Scale bar* 1 mm. *Error bars* ±standard deviation of the mean of 4 slices. These images show that **2** and **3** produce the greatest reduction in T_1

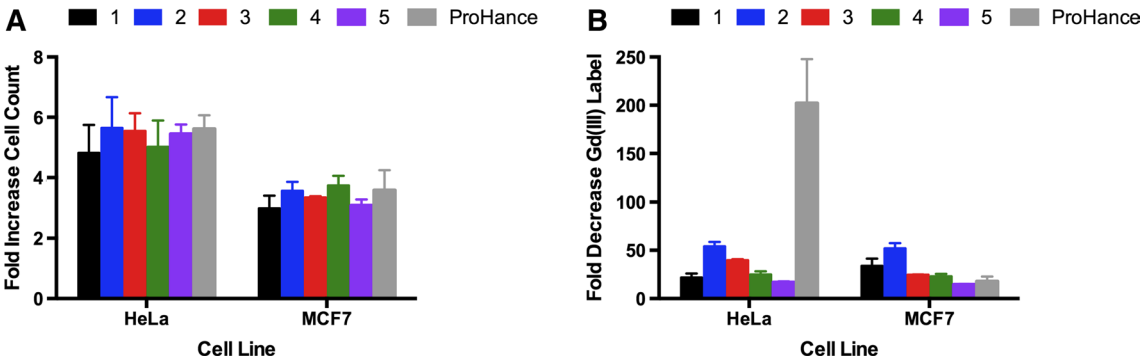

Fig. 4 Cellular proliferation and retention of **1**–**5** and ProHance® in HeLa and MCF7 cells 72 h post-labeling. **a** Cellular proliferation was determined by calculating the fold increase in cell count between t = 0 and 72 h. Data show that complexes **1**–**5** do not slow proliferation. **b** Cellular retention was determined by calculating the fold decrease in Gd(III) per cell between t = 0 and 72 h. These data show that retention is a cell line-dependent property with the lipophilic complexes outperforming ProHance® in HeLa cells but not in MCF7 cells

the greatest image contrast despite having labeling of only 1.17 fmol Gd(III) per cell. Cells labeled with **2** have higher Gd(III) content (2.44 fmol Gd(III) per cell) and the same T_1 as cells labeled with **3** but do not produce as significant T_1-weighted contrast. This may be attributed to some T_2 shortening due to the higher labeling. We believe that this effect is unlikely to be the result of relaxivity changes upon intercalation into the cell membrane because previously lipophilic agents were shown to exhibit the same relaxivity in solution and bound to nanoparticle-cell membrane mimics (called Nanodiscs) [30]. Overall, these data show that while all the lipophilic complexes produce significant contrast compared to cells incubated with ProHance®, complex **3** is the most promising for high-field imaging.

Cellular retention and proliferation

Cellular proliferation and retention of **1**–**5** and ProHance® were determined in HeLa and MCF7 cells by incubation with various concentrations of the agents to equalize Gd(III) per cell labeling. Labeled cells were re-plated in fresh (contrast agent free) media at t = 0 and allowed to proliferate for 72 h. Cell count and Gd(III) labeling were determined at t = 0 and t = 72 h. Cells treated with **1**–**5** showed the same proliferative ability as cells treated with ProHance® (Fig. 4a).

Cellular retention was determined by calculating the fold decrease in cell labeling between t = 0 and 72 h. In HeLa cells, **1**–**5** all have improved cellular retention compared to ProHance® (Fig. 4b). Complexes **1**, **4**, and **5** have the greatest retention with an approximately tenfold improvement compared to ProHance®. Complexes **2** and **3** have a fourfold and fivefold improvement, respectively, compared to ProHance® indicating that the superior cell labeling and MR contrast produced by these complexes does not directly correlate to enhanced cellular retention. In MCF7 cells, complexes **3**, **4**, **5** and ProHance® have similar cellular retention. Surprisingly, the retention of **1** and **2** is lower

than ProHance® suggesting that these complexes are not suited for long-term cell tracking studies in all cell lines.

These data show that cellular retention is dependent upon cell line selection. While the lipophilic complexes provide enhanced retention in HeLa cells, there is no significant enhancement in MCF7 cells. Additionally, complexes **4** and **5** have the most consistent cellular retention in both cell lines despite the lower labeling attained with these agents in 24-h labeling experiments (Fig. 2). This suggests that it may be necessary to sacrifice high cell labeling for improved cellular retention.

Conclusion

We have synthesized five lipophilic Gd(III)-based contrast agents with varied alkyl chain compositions including saturated single alkyl chains (**1** and **2**), unsaturated alkyl chains (**3**), hydrophilic PEG spacer (**4**), and double alkyl chains (**5**). We show that each complex disperses in water, forms micelles in solution, and labels the cell membrane in vitro. Further, we show that there is an inverse relationship between cell labeling and retention where the complexes that label cells most effectively do not have enhanced cellular retention and the complexes that label cells least effectively have the most enhanced cellular retention. These experiments provide guidance for design principles of lipophilic Gd(III)-based MRI contrast agents. To achieve high cell labeling, agents should be synthesized with long alkyl chains and highly positive log*P* values. For improved cellular retention, agents should possess short alkyl chains or hydrophilic spacers. In future work, the mechanisms for label dilution over time and the potential for lipid exchange to cause cell-to-cell jumping of lipophilic contrast agents must be investigated before these agents can be used for long-term cell tracking applications.

Acknowledgments This work was supported by the National Institutes of Health (NIH Grants R01EB005866 and P01HL108795) and by a National Science Foundation Graduate Research Fellowship (C. C.). Imaging was performed at the Northwestern University Center for Advanced Molecular Imaging generously supported by NCI CCSG P30 CA060553 awarded to the Robert H Lurie Comprehensive Cancer Center. MRI was performed on the 7 T Bruker Pharmscan system purchased with the support of NCRR 1S10RR025624-01. Metal analysis was performed at the Northwestern University Quantitative Bioelemental Imaging Center generously supported by NASA Ames Research Center NNA06CB93G.

References

1. Valone FH, Small E, MacKenzie M, Burch P, Lacy M, Peshwa MV, Laus R (2001) Cancer J 7:S53–S61
2. Fernandez-Aviles F, San Roman JA, Garcia-Frade J, Fernandez ME, Penarrubia MJ, de la Fuente L, Gomez-Bueno M, Cantalapiedra A, Fernandez J, Gutierrez O, Sanchez PL, Hernandez C, Sanz R, Garcia-Sancho J, Sanchez A (2004) Circ Res 95;742–748
3. Semsarian C (2002) Intern Med J 32:259–265
4. Petit-Zeman S (2001) Nat Biotechnol 19:201–206
5. Marr RA, Thomas RM, Peterson DA (2010) Future Neurol 5:527–541
6. Webb GA (2006) Modern magnetic resonance. Springer, Dordrecht
7. Rogers WJ, Meyer CH, Kramer CM (2006) Nat Clin Pract Card 3:554–562
8. Caravan P, Ellison JJ, McMurry TJ, Lauffer RB (1999) Chem Rev 99:2293–2352
9. Merbach AE, Tóth E (2001) The chemistry of contrast agents in medical magnetic resonance imaging. Wiley, Chichester
10. Daldrup-Link HE, Rudelius M, Metz S, Piontek G, Pichler B, Settles M, Heinzmann U, Schlegel J, Oostendorp RAJ, Rummeny EJ (2004) Eur J Nucl Med Mol Imaging 31:1312–1321
11. Allen MJ, MacRenaris KW, Venkatasubramanian PN, Meade TJ (2004) Chem Biol 11:301–307
12. Endres PJ, MacRenaris KW, Vogt S, Meade TJ (2008) Bioconjugate Chem 19:2049–2059
13. Wunderbaldinger P, Josephson L, Weissleder R (2002) Bioconjugate Chem 13:264–268
14. Modo M, Cash D, Mellodew K, Williams SCR, Fraser SE, Meade TJ, Price J, Hodges H (2002) Neuroimage 17:803–811
15. Modo M, Mellodew K, Cash D, Fraser SE, Meade TJ, Price J, Williams SCR (2004) Neuroimage 21:311–317
16. Liu Y, He ZJ, Xu B, Wu QZ, Liu G, Zhu HY, Zhong Q, Deng DY, Ai H, Yue Q, Wei Y, Jun S, Zhou GQ, Gong QY (2011) Brain Res 1391:24–35
17. Hsiao JK, Tsai CP, Chung TH, Hung Y, Yao M, Liu HM, Mou CY, Yang CS, Chen YC, Huang DM (2008) Small 4:1445–1452
18. Terreno E, Crich SG, Belfiore S, Biancone L, Cabella C, Esposito G, Manazza AD, Aime S (2006) Magn Reson Med 55:491–497
19. Di Gregorio E, Gianolio E, Stefania R, Barutello G, Digilio G, Aime S (2013) Anal Chem 85:5627–5631
20. Zheng Q, Dai HQ, Merritt ME, Malloy C, Pan CY, Li WH (2005) J Am Chem Soc 127:16178–16188
21. Carney CE, MacRenaris KW, Mastarone DJ, Kasjanski DR, Hung AH, Meade TJ (2014) Bioconjugate Chem 25:945–954
22. Song Y, Kohlmeir EK, Meade TJ (2008) J Am Chem Soc 130;6662–6663
23. Pajk S, Garvas M, Strancar J, Pecar S (2011) Org Biomol Chem 9:4150–4159
24. Basabe P, de Roman M, Marcos IS, Diez D, Blanco A, Bodero O, Mollinedo F, Sierra BG, Urones JG (2010) Eur J Med Chem 45:4258–4269
25. Chalker JM, Gunnoo SB, Boutureira O, Gerstberger SC, Fernandez-Gonzalez M, Bernardes GJL, Griffin L, Hailu H, Schofield CJ, Davis BG (2011) Chem Sci 2:1666–1676
26. Kurniasih IN, Liang H, Mohr PC, Khot G, Rabe JP, Mohr A (2015) Langmuir 31:2639–2648
27. Zheng YR, Suntharalingam K, Johnstone TC, Yoo H, Lin W, Brooks JG, Lippard SJ (2014) J Am Chem Soc 136:8790–8798
28. Li XS, Turanek J, Knotigova P, Kudlackova H, Masek J, Parkin S, Rankin SE, Knutson BL, Lehmler HL (2009) Colloid Surf B 73;65–74
29. New EJ, Congreve A, Parker D (2010) Chem Sci 1:111–118
30. Carney CE, Lenov IL, Baker CJ, MacRenaris KW, Eckermann AL, Sligar SG, Meade TJ (2015) Bioconjugate Chem 26:899–905